Relationships between regional ventilation and vascular and extravascular volume in supine humans

L. H. BRUDIN, C. G. RHODES, S. O. VALIND, T. JONES, B. JONSON, AND J. M. B. HUGHES
Medical Research Centre Cyclotron Unit and Department of Medicine, Royal Postgraduate Medical School, Hammersmith Hospital, London W12 0HS, United Kingdom; and Department of Clinical Physiology, University of Lund, S-221 85 Lund, Sweden

Brudin, L. H., C. G. Rhodes, S. O. Valind, T. Jones, B. Jonson, and J. M. B. Hughes. Relationships between regional ventilation and vascular and extravascular volume in supine humans. *J. Appl. Physiol.* 76(3): 1195–1204, 1994.— With the use of positron emission tomography, alveolar ventilation ($\dot{V}A$), lung density, and pulmonary blood volume (V_B) were measured regionally in eight nonsmokers in the supine posture and one nonsmoker in the prone posture during quiet breathing in a transaxial thoracic section at midheart level. Regional values of alveolar volume (V_A) and extravascular tissue volume (V_{EV}) were derived from the inherent relationships between different compartments in the lung. Ratios proportional to gas volume (V_A/V_{EV}) and ventilation ($\dot{V}A/V_{EV}$) per alveolar unit, respectively, were calculated. No differences between right and left lung were found. Variations in the vertical direction could explain ~65% of the total within-group variation in V_A, V_B, and ln ($\dot{V}A$), whereas the corresponding value for horizontal variation was only 3–9% (right lung, supine subjects). Similar gravitational gradients were found in the single prone subject. There was a significant linear correlation between V_A and ln ($\dot{V}A$). When V_A and $\dot{V}A$ are related to a given number of alveolar units (V_{EV}), the data are consistent with a linear relationship between $\dot{V}A/V_{EV}$ and V_A/V_{EV}, indicating that ventilation might be explained by the elastic properties of lung tissue according to Salazar and Knowles (*J. Appl. Physiol.* 19: 97–104, 1964). Regional V_B was closely associated with the gradient of regional alveolar volume (V_A/V_{EV}) (by virtue of weight of blood and competition for space) and therefore, indirectly, closely associated with the vertical gradient of ventilation.

neon-19; regional alveolar gas volume; regional pulmonary blood volume

REGIONAL DIFFERENCES of ventilation at rest reflect differences in local lung compliance (12, 14), although less so in the prone position (2). These variations in compliance arise due to differences in alveolar expansion under the influence of the weight of the lung (1, 14). There are exceptions to this simplifying hypothesis, particularly in decubitus postures (10). Although Agostoni (1) expressed some doubt, there is persuasive evidence that the vertical gradient of transpulmonary pressure is for the most part related to the weight of the lung (7, 13, 23). Blood contributes more than one-half the weight of the lung (5) and so, indirectly, contributes to the vertical gradient of alveolar expansion and ventilation. The effect of the disposition of vascular weight, from lung top to bottom, on the gradient of pleural pressure and alveolar expansion is not known from either theory (23, 24) or experiments.

In this study, the topography of alveolar ventilation ($\dot{V}A$), alveolar volume (V_A), blood volume (V_B), and gas content and ventilation per milliliter of lung tissue [V_A and $\dot{V}A$ per unit extravascular volume (V_{EV})] have been measured in absolute units (ml or ml/min per cm^3 thorax or per ml lung tissue) in supine normal subjects by using positron emission tomography (PET).

PET offers good spatial resolution in three dimensions and a precise definition of radioisotopic concentrations within a specified geometry. Because lung density (D_L), V_B, and $\dot{V}A$ are measured in absolute and not relative units, relationships between them can be explored. The number of alveolar units varies between regions because of regional differences in gas volume and the influence of the vascular compartment through competition for space. The performance of individual alveolar units in a given region may be studied by normalizing the measured parameters to V_{EV} under the assumption that the alveolar structure in terms of tissue volume does not differ between regions.

This study of humans concentrates on the supine posture, but data from one prone subject are included. It centers on the association between V_B and V_A, on the one hand, and between V_A and $\dot{V}A$ at the alveolar level, on the other hand. Parts of the analysis were designed to investigate whether the data were consistent with the hypothetical exponential pressure-volume (P-V) curve first described by Salazar and Knowles (19).

MATERIALS AND METHODS

Subjects

Eight healthy nonsmoking subjects were studied in the supine posture, and a different subject was studied in the prone posture (Table 1). The study was approved by the Hammersmith Hospital Research Ethics Committee and the United Kingdom Administration of Radioactive Substances Advisory Committee.

PET

PET is a noninvasive technique used to measure the distribution of radionuclides in tomographic sections of the body. Subjects can be studied under physiological and relaxed conditions with unimpeded breathing. Because of the short half-life of the tracers, sequential scans can be recorded at the same session with the subject maintained in a carefully preserved position without changes in counting geometry.

The ECAT II scanner used (CTI, Knoxville, TN) is a single-plane machine with a spatial resolution of 1.7 cm full width at half maximum (16). In transmission mode, the quantitative topographical distribution of D_L is obtained (5, 17). Reconstruction of tomograms were made as described (18) except that D_L was corrected for a small systematic overestimation (0.026 g/cm^3) obtained from phantom studies (5, 17). The transmission measurement was also used to correct subsequent emission

TABLE 1. *Subject data*

Subj No.	Sex	Age, yr	Height, cm	Weight, kg
		Supine subjects		
1	F	39	166	52
2	M	29	185	70
3	M	25	179	72
4	M	28	188	80
5	M	33	170	64
6	M	31	170	84
7	M	33	181	77
8	F	55	168	60
Mean ± SD		34±9	176±8	70±11
		Prone subject		
	M	37	186	74

scans for losses due to attenuation of the emitted photons. In emission mode, tomograms provide the quantitative topographic distributions of isotope concentration.

Computation of Physiological Parameters

V_A. V_A (ml/cm^3 thorax) is obtained from the relationship

$$V_A = 1 - D_L/1.04 \quad (1)$$

where D_L is the total lung density (g/cm^3; lung + blood) and 1.04 g/cm^3 is the density of gas-free lung (21).

V_B and tissue volume. V_B was measured after the inhalation of ^{11}CO (5, 6, 18). Simultaneous measurement of peripheral venous whole blood ^{11}CO concentration allows the calculation of pulmonary V_B (ml/cm^3 thoracic volume). The thoracic volume element comprises V_A (ml gas/cm^3 thorax), V_B (ml blood/cm^3 thorax), and V_{EV} (ml blood-free lung/cm^3 thorax). V_{EV} is, therefore, obtained by

$$V_A + V_B + V_{EV} = 1$$

or

$$V_{EV} = D_L/1.04 - V_B \quad (2)$$

On the assumption that extravascular fluid per alveolus is constant (20) and that the alveolar structure in terms of solid tissue is homogeneous throughout the lung in normal (nonsmoking) subjects, V_{EV} is proportional to the number of alveoli per unit of thoracic volume. The relative volume of gas per alveolar unit can therefore be estimated by V_A/V_{EV} (ml gas/cm^3 tissue) (5).

$\dot{V}A$. Measurements of $\dot{V}A$ were made at steady state during continuous inhalation of the inert short-lived isotope ^{19}Ne (decay constant = 2.39 min^{-1}) (21, 22)

$$\dot{V}A = V_A/[V_A/(S_{^{19}Ne}/C_I) - 1] = V_A/(C_I/C_A - 1) \quad (3)$$

This equation is based on the balance between delivery of tracer to the alveoli by ventilation ($C_I\dot{V}A$) and elimination by ventilation ($C_A\dot{V}A$) and decay (C_AV_A). C_I is the concentration of ^{19}Ne in the inspired air, and C_A is the regional concentration of ^{19}Ne in alveolar gas and is calculated as ^{19}Ne concentration per cubic centimeter of thorax from the emission scan ($S_{^{19}Ne}$) divided by V_A. In addition, $\dot{V}A$ expressed per unit V_{EV} ($\dot{V}A/V_{EV}$) was calculated.

Protocol

Measurements were made in a single transverse section through the thorax, at midheart level, with the subject in the supine posture. A different subject was studied prone. After three or four short transmission scans were recorded at different levels above the diaphragm to localize where the right heart contour was most prominent, a 10-min transmission scan was made to measure regional D_L and regional V_A. A 400-s emission scan was then recorded during the continuous inhalation of ^{19}Ne in a gas mixture (25–33% O_2-67–75% N_2). The subject inhaled ^{11}CO (~330 MBq) to label the red blood cell pool, after which 3–4 min were allowed for mixing before a single 10-min emission scan was recorded and blood ^{11}CO concentration measured. During the whole study (~2 h), the subject maintained a carefully preserved position, which was checked with a light grid projected onto the chest.

Data Analysis and Error Considerations

Because of limited resolution, isotope concentration at the periphery of the lung close to the pleural surface cannot be measured accurately. The values of D_L at the periphery are influenced by the high density of surrounding tissues, and the values of pulmonary V_B are influenced by the high V_B within the heart and central vessels. These boundaries set the limits within which the structural and functional parameters can be reliably quantified. With a thresholding procedure (5) a 2-cm strip of the periphery of each lung was exempted from analysis as were the hilar regions (Fig. 1). Regional values of the parameters were then obtained for the right and left lungs by calculating the mean values per unit area in each of 1.3 × 1.3-cm square regions covering the lung fields in the chosen plane. The total number of regions was 267, ranging between 25 and 44 per individual. The vertical and horizontal distances were measured relative to the center of the right ventricle and peripheral (lateral) lung border, respectively.

With sufficient tracer activity and duration of the scanning time, the statistical error in the measurement of D_L is on the order of 0.01–0.02 g/cm^3 [the coefficient of variation (CV) of V_A is ~3.5% in a resolution element (2.9 cm^2) (21)], and in the measurements of tracer activity it is on the order of 2–4%. The statistical uncertainty in the measurement of tracer activity in samples of blood and gas is kept at negligible levels (in comparison to other errors) by using sufficiently long counting time.

Errors due to simplifications in the underlying theory of the ^{19}Ne model are, in normal lung, mainly due to dead space ventilation. In poorly ventilated regions (ventral) the fresh gas $\dot{V}A$ is overestimated by ~2–3%, whereas there is ~8% underestimation in regions with highest ventilation (dorsal) (22). The calculation of $\dot{V}A$ from the steady-state flow equation tends to amplify the statistical noise, especially in regions with high ventilation. For the low-ventilation regions, CV of $\dot{V}A$ is on the order of 5–6%, whereas these random errors amount to 10–12% in the best-ventilated regions (21). V_{EV} constitutes the relatively small difference between two measurements, D_L and V_B, each affected by statistical errors. This results in an increased uncertainty in the values of V_{EV} obtained, and the CV of V_{EV} may be on the order of 20–30% in individual regions.

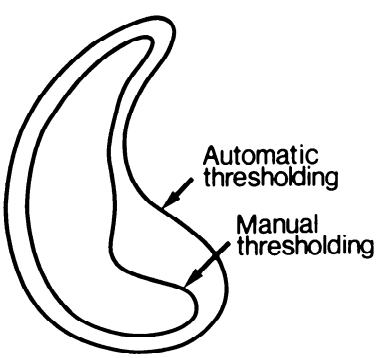

FIG. 1. Data analysis (for right lung). Coarse thresholding removed all pixels from density image with values >0.75 g/cm^3; further thresholding followed by hand.

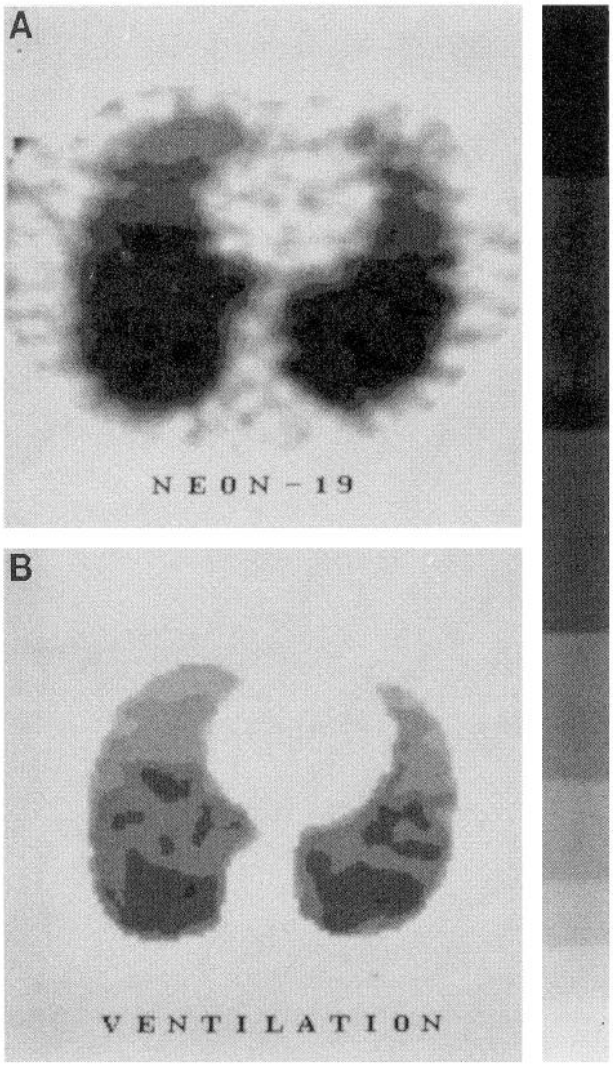

FIG. 2. Tomograms from 1 supine subject, showing regional concentration (Bq/cm^3 thorax) of ^{19}Ne ($S_{^{19}Ne}$) (*A*), from which distribution of alveolar ventilation ($\dot{V}_A$) has been calculated (*B*). Logarithmic scale has been used. Top of scale is 1.5 ml · min^{-1} · cm^{-3} for $\dot{V}_A$.

Vertical and horizontal variation. Because of differences in lung size between subjects, relationships based on the topographical variations of the parameters (vertical and horizontal) were studied by the method of multiple regression (polynomials) in groups (8 supine subjects) and using dummy variables (3). The method allows the explained variation in horizontal and vertical directions to be estimated in relation to the within-group (subjects) variation, as well as individual differences in regression parameters and mean values. $P > 0.05$ has been regarded nonsignificant, and $P < 0.001$ was the lowest level used. The correlation coefficients (R) were calculated as *1)* R(common) = $\sqrt{\text{explained variation due to common regression/total variation within groups}}$ and *2)* R(individual) = $\sqrt{\text{explained variation due to individual regression/total variation within groups}}$ (2). Data from the prone subjects are dealt with separately.

Interparametrical relationships. The calculated values of $\dot{V}_A$, V_A, and V_{EV} are to some extent interdependent, since they are all derived from the same basic set of measurements (D_L, V_B, and $S_{^{19}Ne}/C_I$). Random errors in these measurements affect the correlations between the calculated parameters. To avoid this, interparametrical relationships have been explored indirectly. Thus the relationship between $\dot{V}_A$ and V_A was explored by relating the independent measurements of $S_{^{19}Ne}/C_I$ and V_A by the method of multiple regression in groups (see above).

The elastic properties of lung tissue are expressed in the relationship between V_A/V_{EV} and $\dot{V}_A/V_{EV}$. This relationship, however, could not be tested directly due to the strong coupling between the two parameters and the high noise level in the determination of V_{EV}. Instead, a hypothesized P-V curve was used together with the experimentally determined relationship between $\dot{V}_A$ and V_A to predict the interdependence between V_B and V_A (see *Eq. 2*). This relationship was then tested (multiple regression in groups for supine subjects; see above) using observed values of V_B and V_A, which were independently measured.

Normalization of data in graphs. To graphically illustrate topographical and in some cases interparametrical trends, differences between supine subjects in the average levels of the parameters were compensated for by normalizing the individual mean to the group mean. The reason for this is the substantial differences in mean values between subjects, especially $\dot{V}_A$. This was done by multiplying regional values in each subject by $M(x)/Mi(x)$, where $Mi(x)$ is the individual mean value (right lung slice) of *parameter x* and $M(x)$ is the overall group mean value. Data for the prone subject are shown separately.

RESULTS

Figure 2 shows images of ^{19}Ne concentration (*A*) and the derived tomogram of $\dot{V}_A$ (*B*). Individual mean values

TABLE 2. *Mean values of structural parameters and regional ventilation*

Subj No.	V_A, ml/cm^3	V_B, ml/cm^3	V_{EV}, ml/cm^3	$\dot{V}_A$, ml · min^{-1} · cm^{-3}	V_A/V_{EV}, ml/ml	$\dot{V}_A/V_{EV}$, ml · min^{-1} · ml^{-1}
			Supine subjects			
1	0.68	0.20	0.12	1.8	5.6	14.0
2	0.76	0.15	0.09	2.2	8.3	24.1
3	0.75	0.16	0.10	1.8	7.5	17.4
4	0.76	0.16	0.07	0.8	11.3	11.4
5	0.73	0.17	0.11	0.7	7.1	6.7
6	0.67	0.17	0.16	1.1	4.4	6.8
7	0.69	0.19	0.13	2.2	6.3	17.6
8	0.70	0.16	0.14	0.8	5.2	6.1
Mean ± SD	0.72±0.04	0.17±0.02	0.12±0.03	1.4±0.6	7.0±2.1	13.0±6.5
			Prone subject			
	0.70	0.15	0.15	0.81	4.9	5.7

V_A, alveolar gas volume; V_B, fractional blood volume; V_{EV}, extravascular tissue volume; $\dot{V}_A$, alveolar ventilation; V_A/V_{EV}, lung expansion; $\dot{V}_A/V_{EV}$, ventilation per alveolar unit for right lung slice.

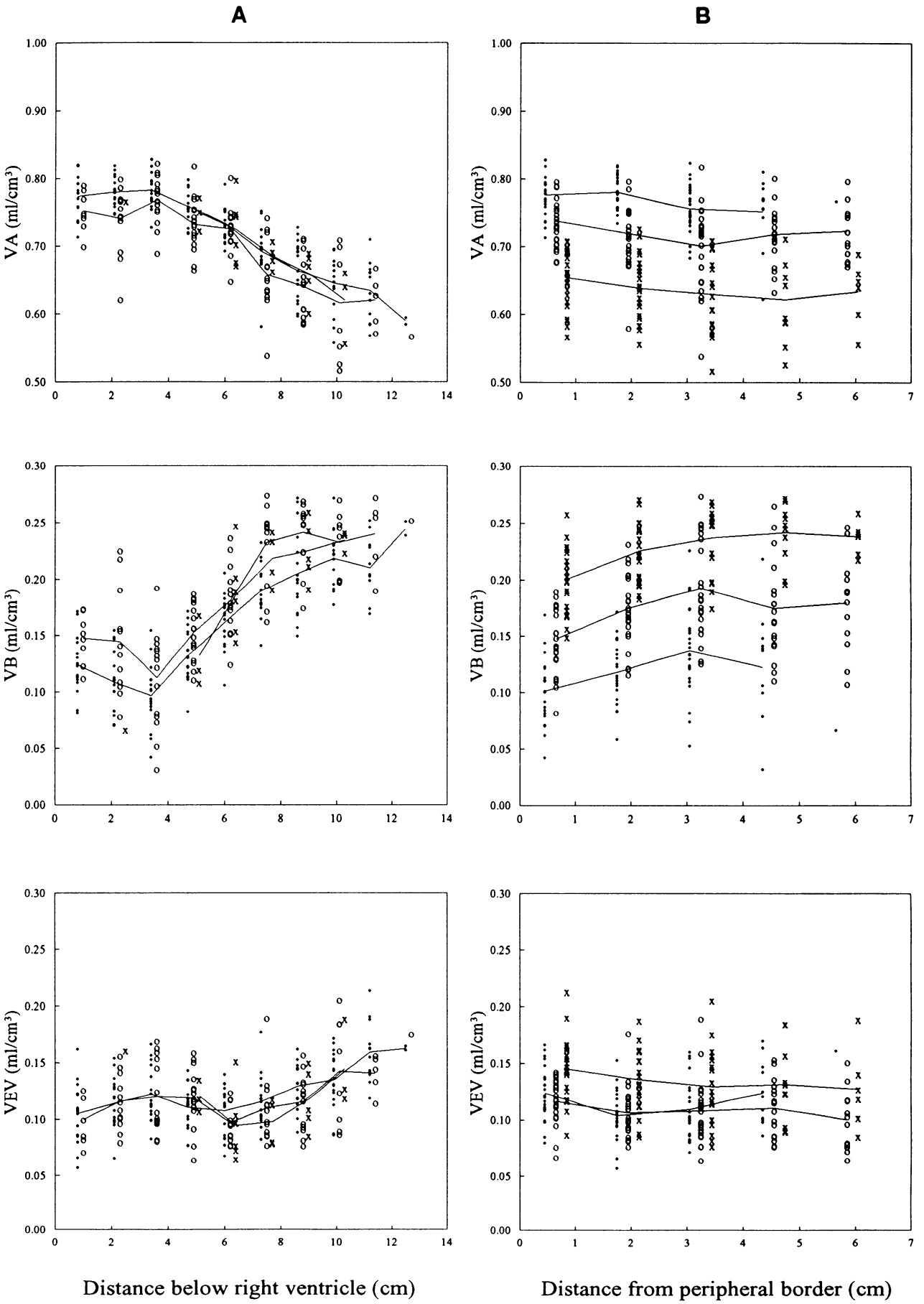

TABLE 3. *Relationships between various parameters (right lung) and vertical and horizontal levels*

	V_A, ml/cm³	V_B, ml/cm³	V_{EV}, ml/cm³	$S_{^{19}Ne}/C_I$	ln($\dot{V}_A$)	V_A/V_{EV}, ml/ml	$\dot{V}_A/V_{EV}$, ml·min⁻¹·ml⁻¹
α	0.79	0.09	0.11	0.27	−0.15	7.54	8.61
β of x_1							
$\beta(x_1)$		−0.0238		0.0095	0.0851		−1.3096
$\beta(x_1^2)$	−0.0016	0.0084					0.6950
$\beta(x_1^3)$		-4.9×10^{-4}	3.9×10^{-5}			−0.0028	−0.0494
β of x_2							
$\beta(x_2)$	−0.0069	0.0255		0.0112	0.0926		2.9893
$\beta(x_2^2)$		−0.0029		−0.0031	−0.0218		−0.5963
R^2(common)	0.67	0.73	0.22	0.65	0.70	0.24	0.45
R^2(individual) regression	0.80	0.86	0.35	0.73	0.79	0.32	0.74
r^2(vertical)	0.66	0.66	0.22	0.53	0.65	0.24	0.36
r^2(horizontal)	0.03	0.08		0.18	0.09		0.16

Values are from 8 supine subjects and were calculated by multiple regression in groups. Total number of regions = 267. $S_{^{19}Ne}/C_I$, ratio of regional pulmonary concn of ^{19}Ne by emission scan to concn of ^{19}Ne in inspired air; x_1, cm below right ventricle; x_2, cm from peripheral edge of lung; α, intercept; β, partial regression coefficient; R, multiple correlation coefficient; r, partial correlation coefficient. Note that difference between R^2(common) and R^2(individual) is caused by differences in β values between subjects. Because of small interdependence between x_1 and x_2, sum of r^2(vertical) and r^2(horizontal) exceeds R^2(common).

for the right lung of the structural parameters (V_B, V_{EV}, V_A, and V_A/V_{EV}) and regional ventilation ($\dot{V}A$, $\dot{V}A/V_{EV}$) are shown in Table 2. When comparisons were made at the same vertical height, no significant differences were found between the right and left lungs. Mean values for the supine subjects (SD between subjects) of the right-to-left ratios were 0.98 (0.10) for V_B, 0.93 (0.15) for V_{EV}, 1.02 (0.02) for V_A, and 1.01 (0.15) for $\dot{V}A$.

No correlations were found between age and V_{EV}, V_B, or $\dot{V}A$.

Vertical and Horizontal Gradients

Supine subjects. The gradients for V_A, V_B, and V_{EV} are shown in Fig. 3, and the regression parameters and correlation coefficients are given in Table 3 (only significant polynomials are included). In the ventral one-third (for V_B) and in the ventral one-half (for V_{EV}), no vertical gradients were seen in any of the subjects, as previously described (5, 18). There were significant but small horizontal gradients at these vertical levels (Fig. 3*B*, Table 3) for V_A and V_B but not for V_{EV}. Of the regional variation in V_A and V_B, 66% could be explained by a gravity-dependent process [Table 3, r^2(vertical)] and only 3 and 8%, respectively, by a gravity-independent mechanism [Table 3, r^2(horizontal)]. Only 22% of the variation in V_{EV} was caused by systematic changes in the vertical axis.

Figure 4 plots vertical (*A*) and horizontal (*B*) gradients for $\dot{V}A$ per unit thoracic volume [ln ($\dot{V}A$)] and the unmanipulated regional ^{19}Ne concentration (normalized for C_I). Both indexes show the same trends, with $\dot{V}A$ increasing from ventral to dorsal and from medial to lateral. Of the variation in ln ($\dot{V}A$), 65% [Table 3, r^2(vertical)] can be explained by a gravity-dependent gradient and 9% [Table 3, r^2(horizontal)] by a gravity-independent gradient. When the data are manipulated by dividing $\dot{V}A$ by V_{EV} to show ventilation per unit tissue volume (or per alveolus), the vertical and horizontal gradients account for only 36 and 16%, respectively, of the variation, illustrating the influence of alveolar number and/or alveolar size (volume) on local $\dot{V}A$.

All parameters in Table 3 showed significant differences in the regression coefficients between subjects. Except for $\dot{V}A/V_{EV}$, the differences in R^2 for all subjects taken together (group regression) and for all subjects separately (individual regression) were small.

Prone subject. The gradients for V_A and V_B and for $\dot{V}A$ [ln ($\dot{V}A$)] are shown in Fig. 5. All three parameters showed significant changes in the vertical axis [$P < 0.001$ for V_B and ln ($\dot{V}A$) and $P < 0.005$ for V_A]. There were significant horizontal trends in V_B ($P < 0.02$) and V_A ($P < 0.001$) but not in $\dot{V}A$.

Relationship Between Regional $\dot{V}A$ and Regional V_A or V_B

A preliminary analysis was first made by plotting normalized values of the logarithm of local $\dot{V}A$ per cubic centimeter of thorax against local expansion (V_A) (Fig. 6*B*). This relationship appeared to be linear, but the data were subject to the effect of a weak mathematical coupling between $\dot{V}A$ and V_A (*Eq. 3*), which could have resulted in a pseudocorrelation. To circumvent this problem the following procedure was adopted. The primary data, $S_{^{19}Ne}/C_I$ (normalized) and V_A (which are measured independently), were subjected to a polynomial regression analysis (Fig. 6*A*) giving

$$S_{^{19}Ne}/C_I = a_0 + a_1V_A + a_2V_A^2 \quad (4)$$

where a_0, a_1, and a_2 are constants. For any value of V_A, $S_{^{19}Ne}/C_I$ can thus be calculated (free from pseudocorrela-

FIG. 3. Vertical (*A*) and horizontal (*B*) profiles of alveolar gas (V_A), fractional blood (V_B), and extravascular tissue volumes (V_{EV}). For each of 8 supine individuals, values were normalized to common mean calculated for all 8 subjects to exhibit vertical and horizontal trends. For each vertical level (*A*), data were separated into 3 subgroups: horizontal levels <2 cm from peripheral lung edge (solid circles), 2–5 cm (open circles), and >5 cm (crosses). Similarly, for each horizontal level (*B*), 3 subgroups were chosen: vertical levels <3 cm below right ventricle (solid circles), 3–7 cm (open circles), and >7 cm (crosses). Mean values for each subgroup and level are connected by straight lines.

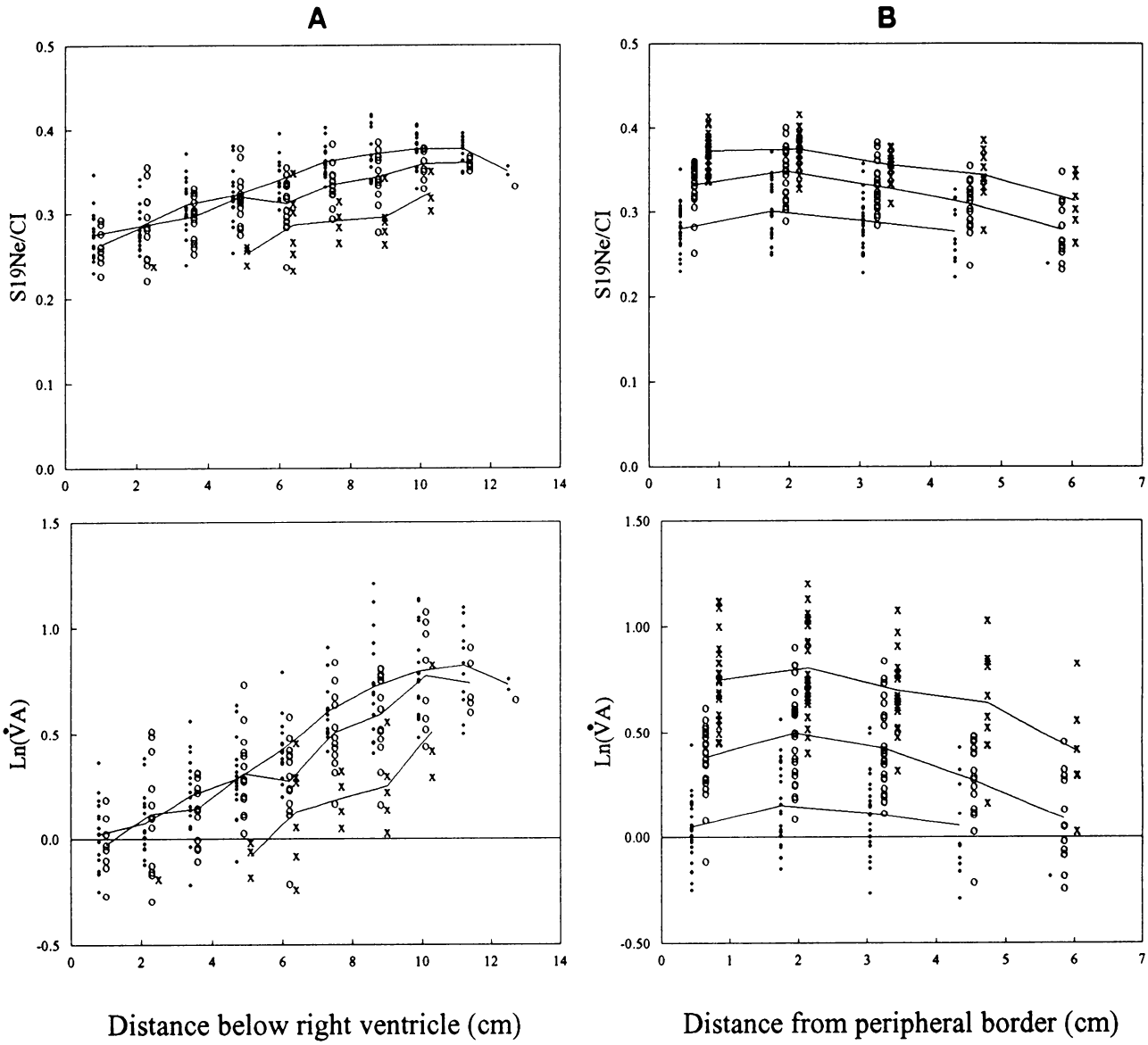

FIG. 4. Vertical (*A*) and horizontal (*B*) profiles of $S_{^{19}Ne}$-to-concentration of ^{19}Ne in inspired air (C_I) ratio and $\dot{V}A$ ($ml \cdot min^{-1} \cdot cm^{-3}$) calculated for supine subjects. For explanation see Fig. 3 legend.

tion, *Eq. 4*) and ln ($\dot{V}A$) determined from *Eq. 3*. The solid line in Fig. 6*B*, which results from this procedure, is almost linear and fits closely to measured data points [in actual fact, a linear regression of ln ($\dot{V}A$) vs. V_A gives a straight line that is superimposable on the curve shown]. The finding that the relationship between ln ($\dot{V}A$) and V_A is effectively linear allows the following equation to be written

$$\ln (\dot{V}A) = c_1 - c_2 V_A \quad (5)$$

where c_1 and c_2 are constants. Combining *Eqs. 3* and *5* gives

$$S_{^{19}Ne}/C_I = (2.39 c_0 e^{c_2 V_A} + 1/V_A)^{-1} \quad (6)$$

where $c_0 = e^{-c_1}$. In the following analysis c_0 and c_2 were optimized by the method of multiple regression in groups (supine subjects, Table 4; not normalized data). The graph of the linear regression equation for the prone subject is shown separately ($n = 42$, $r^2 = 0.31$, $P < 0.001$; Fig. 6*B*).

To the extent that *1*) the elastic properties of the normal lung are described by a single-exponential function as described by Salazar and Knowles (19) and 2) during tidal breathing the distribution of ventilation is determined primarily by local lung compliance, local ventilation per alveolus will be linearly related to local alveolar expansion (see APPENDIX A for explanation). Figure 6*B* shows that $\dot{V}A$ per cubic centimeter of thorax is exponentially (not linearly) related to V_A per cubic centimeter of thorax, but this does not contradict the prediction of Salazar and Knowles because regions with different alveolar number (i.e., V_{EV}) are being compared. Because the P-V curve analysis of Salazar and Knowles applies to regions with constant alveolar number, it follows that $\dot{V}A$ and V_A, both divided by V_{EV}, should be linearly related if the prediction of Salazar and Knowles is correct. In fact, the relationship between local $\dot{V}A/V_{EV}$ and V_A/V_{EV} is linear as predicted; because of pseudocorrelation and coupling (weak) between $\dot{V}A$ and V_A (*Eq. 3*), this plot has not been shown. Instead, because $V_{EV} = 1 - V_B - V_A$, the

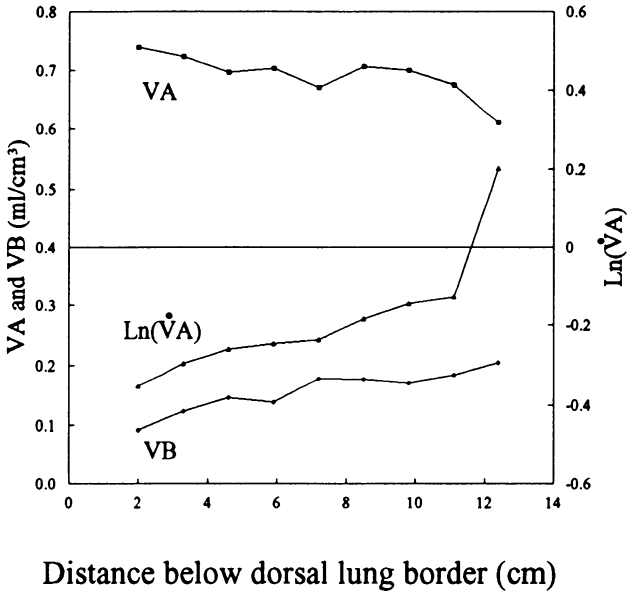

FIG. 5. Vertical profiles of V_A, V_B, and ln ($\dot{V}A$) (where $\dot{V}A$ is expressed in ml · min^{-1} · cm^{-3}) calculated for prone subject. Only mean values at each vertical level are shown and are connected by straight lines.

empirical relationship between V_A and $\dot{V}A$ (*Eq. 5*) can be utilized to predict the relationship between V_A and V_B (see APPENDIX B)

$$V_B = 1 - d_1 V_A - d_2 e^{-c_2 V_A} \quad (7)$$

where d_1 and d_2 include the constants of the P-V curve of Salazar and Knowles. c_2 is given by the V_A-$\dot{V}A$ relationship, whereas d_1 and d_2 are determined by the method of multiple regression in groups (Table 4, supine subjects; Fig. 7). The correlation, shown for all regions in Fig. 7, was highly significant in each subject. Table 4 (supine subjects) gives the constants for *Eqs. 5* and *7* and the group (common) and individual regression coefficients. For the prone subject (n = 42), r^2 = 0.49 ($P < 0.001$).

From *Eqs. 5* and *7* and Table 4, the relationship between V_B and $\dot{V}A$ for the supine subjects can be calculated

$$V_B = 0.16 + 0.27 \ln (\dot{V}A) - 0.05\dot{V}A \quad (8)$$

The individual values and the predicted regression curve are plotted in Fig. 8 [R^2(common) = 0.49 and R^2(individual) = 0.54] together with the regression equation calculated for the prone subject (n = 42, r^2 = 0.35, $P < 0.001$).

DISCUSSION

Mean Values

Mean values of V_A, V_B, V_{EV}, and $\dot{V}A$ expressed per cubic centimeter of thorax calculated for the right lung slice (Table 2) are similar to previous studies using this technique (5, 18, 25). We have previously discussed (5) that if the midthoracic transaxial plane is representative of the lung as a whole and if a total V_A in the supine posture of 2.7 liters is assumed, we obtain a value of total thoracic volume of 3.7 liters and a total lung mass of 1,000 ml comprising 60% blood and 40% V_{EV}. These values are not unreasonable. Total $\dot{V}A$ would be on average 5.2 l/min.

Vertical and Horizontal Gradients

Data for vertical gradients in V_A, V_B, and V_{EV} confirm previous results from our laboratory (5, 18, 25), but a systematic search for horizontal gradients has not previously been made. The diminishing gradients of V_B from central to peripheral parts of the lung slice would be consistent with a similar gradient of pulmonary blood flow and vascular resistance (9). Nevertheless, with the exception of the supine anesthetized dog (8), central-to-peripheral gradients of pulmonary blood flow are relatively small in relation to vertical gradients (11), and the same holds for gradients of pulmonary V_B (Fig. 3). There appears to be a significant increase in regional ventilation in the lung periphery compared with the central parts

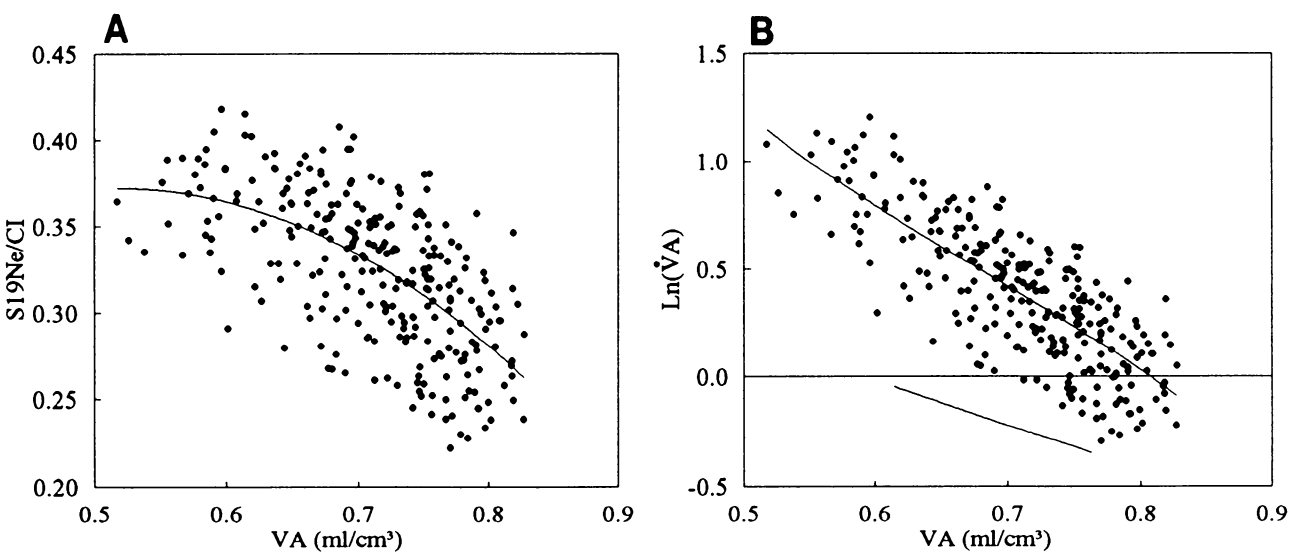

FIG. 6. *A*: relationship between S_{19Ne}/C_I and local V_A (=1 − lung density) for all subjects. For S_{19Ne}/C_I, mean for right lung in each individual was normalized to group mean. Quadratic polynomial fit is shown (solid line; higher orders were not significant). *B*: relationship between ln ($\dot{V}A$) (ml · min^{-1} · cm^{-3}; calculated from *Eq. 3*) and V_A fitted with same polynomial as in *A*. Linear relationship for prone subject is shown separately (bottom line). See text for details.

TABLE 4. *Predicted relationships between ln($\dot{V}_A$) and V_A*

$\ln(\dot{V}A) = c_1 - c_2V_A$				$V_B = 1 - d_1V_A - d_2e^{-c_2V_A}$			
c_1	c_2	R^2(com)	R^2(ind)	d_1	d_2	R^2(com)	R^2(ind)
3.08	3.88	0.64	0.67	1.06	1.09	0.84	0.85

Values are from 8 supine subjects. Total number of regions is 267. Predicted relationship between ln($\dot{V}_A$) and V_A obtained from relationship between V_A and $S_{19_{Ne}}/C_I$ because of small mathematical coupling between $\dot{V}_A$ and V_A (see text); relationship between V_B and V_A calculated by multiple regression in groups. R(com) and R(ind), multiple regression coefficients due to common and individual regression, respectively. Note that c_2 values in V_B-V_A relationship are individually obtained from ln($\dot{V}_A$)-V_A relationship. Difference between R^2(com) and R^2(ind) is caused by differences in regression coefficients between subjects. Pooled data are shown in Figs. 6 and 7. $P < 0.001$ for both equations.

(Fig. 4), and the horizontal gradient of $\dot{V}A/V_{EV}$ (Table 3) contributes one-half as much as the vertical gradient to the overall pattern of regional ventilation. The reason for the horizontal gradient of ventilation is not clear.

In the vertical axis, the most striking finding is a reversal in the gradient of pulmonary V_B in the ventral regions adjacent to the heart in the supine subjects (Fig. 3). This was accompanied by a loss of the vertical gradient for V_A (independent of the V_B measurement) and pulmonary V_{EV} (but not ventilation) in the same region. The relationship between V_B and V_A in the ventral regions follows the same pattern as in the rest of the lung (Fig. 7), which suggests that there is a subtle reversal in the gradient of local expansion (V_A); possibly the lung is being compressed between the heart and the chest wall. Further measurements of different craniocaudal levels are planned to see whether there is a local or general effect. In the prone subject, V_B showed a more continuous increase in the direction of gravity (Fig. 5).

Relationships Between V_A, V_B, and V_{EV}

V_{EV} may be regarded as a measure of the number of alveolar units per unit volume of thorax, provided that the tissue volume of individual alveolar units (free from

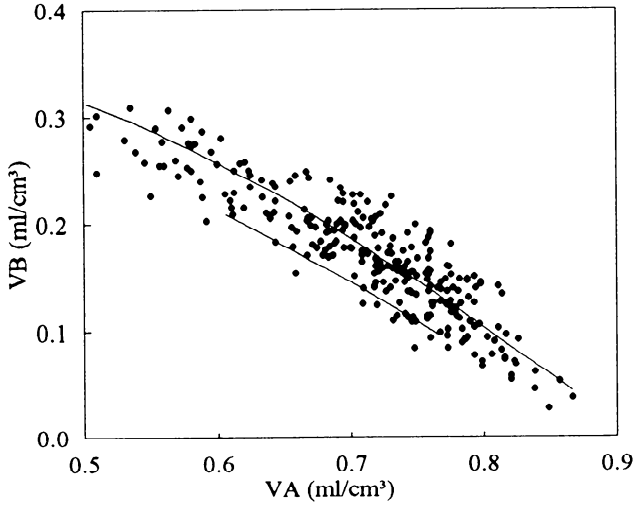

FIG. 7. Relationship between regional V_B and V_A. Regression equation is given by *Eq. 7* (see Table 4). Regression line for prone subject is also shown (bottom line).

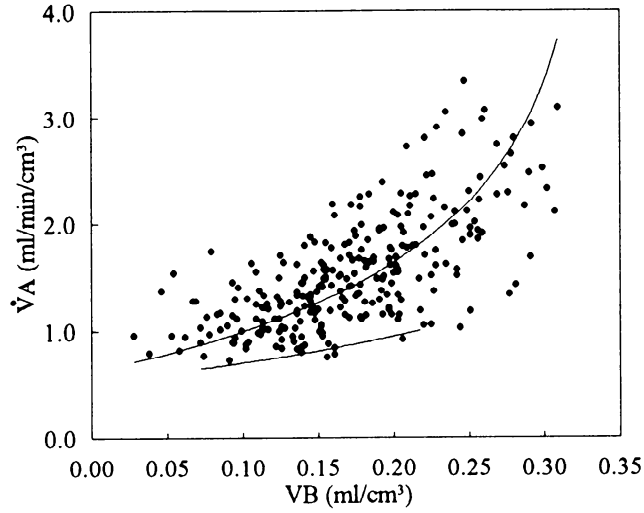

FIG. 8. Relationship between $\dot{V}_A$ and V_B. Values of $\dot{V}_A$ are, for each subject, normalized to group mean ($\dot{V}_A$ = 1.44 ml · min^{-1} · cm^{-3}) to compensate for substantial interindividual variation in $\dot{V}_A$. Note that continuous line, representing *Eq. 8*, is obtained using nonnormalized data. Regression curve for prone data is also shown (bottom line). See text for details.

blood) does not change between regions in healthy lung. Thus, despite the reduction in available space (due to an increased V_B), the number of alveoli per unit volume of thorax is ~30% higher in the dependent part as in the nondependent part of the lung, as indicated by the ventrodorsal distribution of V_{EV}. The sum of V_A, V_B, and V_{EV} constitutes the thoracic volume element (*Eq. 2*). Because of competition for space, all three parameters are interrelated (Fig. 7). For example, a change in V_A from 0.60 to 0.75 ml/cm^3 is associated with a change in V_B of 70% and, thus, with a change in V_{EV} of 30%.

In any region, V_A per cubic centimeter of thorax is the product of the number of alveolar units and the gas volume per alveolar unit. In the lung periphery, which is dominated by alveoli, the alveolar number is assumed to be proportional to V_{EV} and the volume of gas per alveolar unit to V_A/V_{EV} (lung expansion or alveolar size). V_A/V_{EV}, which mathematically is a function of V_B and V_{EV} (*Eq. 2*), falls with increasing V_B and with increasing number of alveoli (V_{EV}). The magnitude by which regional variations in V_B and V_{EV} (ΔV_B and ΔV_{EV}, respectively) are associated with regional variations in V_A/V_{EV} [$\Delta(V_A/V_{EV})$] can be determined by differentiating V_A/V_{EV} with respect to V_B and V_{EV}. Denoting $\Delta y/y$ by the relative change in y between regions (coefficient of regional variation), i.e., CRV(y), we find

$$\mathrm{CRV}(V_A/V_{EV}) = -(1 - V_B)/V_A \cdot \mathrm{CRV}(V_{EV}) - V_B/V_A \cdot \mathrm{CRV}(V_B) \quad (9)$$

or, using mean values for right lung

$$\mathrm{CRV}(V_A/V_{EV}) = -1.15\mathrm{CRV}(V_{EV}) - 0.24\mathrm{CRV}(V_B) \quad (10)$$

If differences in lung expansion were the only cause of the vertical gradients in V_{EV} and V_B, CRV(V_{EV}) would be equal to CRV(V_B). However, analysis of the present data reveals that CRV(V_B) exceeds CRV(V_{EV}) by ~60% when going from ventral to dorsal regions. Thus, regional differences in V_{EV} are associated with 75% of variations in

lung expansion, whereas regional differences in V_B are associated with 25%, according to *Eq. 10*.

The weight of the lung is an important cause of the pleural pressure gradient, which in turn is related to regional lung expansion. The importance of the lung weight as a determinant of the transpulmonary pressure and lung expansion is supported by studies where the lung has been subjected to acceleration (7). Lung weight is about two-thirds blood, i.e., V_B (5). If two-thirds of the gravitational variation of V_{EV} is related to V_B, the influence of V_{EV} on V_A/V_{EV} (75%) can be attributed to V_B in the same proportion. V_B is, therefore, associated with V_A/V_{EV} first by virtue of volume competition (25%) and second by the mechanism of gravity ($0.67 \times 75\% = 50\%$) or 75% in toto. V_{EV} itself is only associated with the gravity variation of V_A/V_{EV} to ~25%.

Relationships Between V_A and V_B and $\dot{V}A$

Figure 6 for the supine subjects and the single prone subject shows that there is a linear relationship between the logarithm of regional $\dot{V}A$ per cubic centimeter of thorax and regional V_A. When $\dot{V}A$ and V_A are each expressed per alveolus (by dividing both by V_{EV}), regional $\dot{V}A$ is linearly related to alveolar expansion (V_A/V_{EV}), as predicted by the expression of Salazar and Knowles (*Eq. 5*; APPENDIX A). Because V_A and V_{EV} together predict V_B (*Eq. 2*) because of competition for space, intuitively V_B must have prediction power for $\dot{V}A$ (Fig. 8; *Eq. 8*). This relationship is internally consistent because the distribution of V_B itself, in terms of its volume and weight (see previous section), is closely associated with V_A and hence with $\dot{V}A$.

These relationships between $\dot{V}A$ and V_B for both supine and prone postures might be explained by the action of gravity on V_B and V_A, but they do not hold in the most ventral portions of the supine lung (Fig. 3). Nevertheless, the important point is that these relationships can only be explored on a regional basis in humans because of the quantification made possible by PET. The companion paper (4) explores the association between V_B and local blood flow on a regional basis. This suggests that mechanical forces, acting largely through gravity, assist matching between regional $\dot{V}A$ and blood flow by virtue of the influence of V_B.

APPENDIX A

Relationship Between Alveolar Expansion and $\dot{V}A$

The V vs. P characteristics of the lung are well described by the exponential function first suggested by Salazar and Knowles (19)

$$V = k_2(1 - k_3e^{-k_4P}) \qquad (A1)$$

where k_2 (volume), k_3 (dimensionless), and k_4 (pressure^{-1}) are constants. This relationship has been shown to fit experimental static P-V relationships in humans in several studies (for review, see Ref. 14). For volume changes during tidal breathing the equation of motion (15) (ignoring inertial forces) is $dP = dV/C + \dot{V}R$, where C is regional pulmonary compliance, $\dot{V}$ is ventilation, and R is airway resistance. During quiet breathing in normal subjects the distribution of inspired gas is predominantly determined by C, and R has therefore been neglected in the following discussion. Thus

$$dV/dP = (dV/dt)/(dP/dt) = \dot{V}/(dP/dt) = C \qquad (A2)$$

where $\dot{V} = dV/dt$ is the absolute change in gas volume per unit of time (=ventilation). Differentiating *Eq. A1* with respect to P gives

$$dV/dP = k_2k_3k_4e^{-k_4P} \qquad (A3)$$

Equations A1, A2, and *A3* give

$$\dot{V} = dP/dt(k_2k_4 - k_4V) \qquad (A4)$$

Under the assumption that the time-dependent change of transpulmonary pressure (dP/d*t*) is uniform throughout the lung

$$\dot{V} = k_1 - kV \qquad (A5)$$

where k_1 [$(dP/dt)k_2k_4$; volume/min] and k [$(dP/dt)k_4$; min^{-1}] are constants, $\dot{V}$ is total ventilation of the lung (lobe or segment) in absolute numbers, and V is the gas volume of the lung (lobe or segment). Thus, on the assumption that *1*) the P-V characteristic is given by *Eq. A1*, *2*) R is negligible, and *3*) dP/d*t* is uniform throughout the lung, $\dot{V}$ (in lung regions with constant alveolar number) is a linear function of V_A. Hence, regarding regions with different mean alveolar size, one would expect mean ventilation per alveolus to be linearly related (with negative slope) to mean alveolar expansion.

APPENDIX B

Derivation of Eq. 7

Salazar and Knowles (19) predicted that (see APPENDIX A)

$$\dot{V}A/V_{EV} = d_3 - d_4V_A/V_{EV}$$

or

$$\dot{V}A = d_3V_{EV} - d_4V_A \qquad (B1)$$

Replacing V_{EV} by $1 - V_A - V_B$ (*Eq. 2*) and solving for V_B gives

$$V_B = 1 - d_1V_A - \dot{V}A/d_3 \qquad (B2)$$

where $d_1 = 1 - d_4/d_3$. However, $\dot{V}A = e^{(c_1 - c_2V_A)}$ (*Eq. 5*), giving

$$V_B = 1 - d_1V_A - (e^{c_1}/d_3)e^{-c_2V_A} \qquad (B3)$$

or

$$V_B = 1 - d_1V_A - d_2e^{-c_2V_A} \qquad (B4)$$

where $d_2 = e^{c_1}/d_3$.

We thank D. D. Vonberg and the staff of the Cyclotron Unit, in particular P. D. Buckingham of the radiochemistry section, for invaluable support and technical and intellectual help and all our volunteers.

This study was supported in part by the Draco Foundation, Thorsten Birger Segerfalks Foundation for Medical Research and Education, Swedish National Association Against Heart Diseases, and Swedish Medical Research Council Grant 02872.

Present address and address for reprint requests: L. H. Brudin, Dept. of Clinical Physiology, Kalmar Hospital, S-391 85 Kalmar, Sweden.

Received 6 April 1992; accepted in final form 12 October 1993.

REFERENCES

1. **Agostoni, E.** Mechanics of the pleural space. In: *Handbook of Physiology. The Respiratory System. Mechanics of Breathing.* Bethesda, MD: Am. Physiol. Soc., 1986, sect. 3, vol. III, pt. 2, chapt. 30, p. 531–559.
2. **Amis, T. C., H. A. Jones, and J. M. B. Hughes.** Effect of posture on inter-regional distribution of pulmonary ventilation in man. *Respir. Physiol.* 56: 145–167, 1984.

3. **Armitage, P.** *Statistical Methods in Medical Research.* London: Blackwell, 1983.
4. **Brudin, L. H., C. G. Rhodes, S. O. Valind, and J. M. B. Hughes.** Interrelationships between regional blood flow, blood volume, and ventilation in supine man. *J. Appl. Physiol.* 76: 1205–1210, 1994.
5. **Brudin, L. H., C. G. Rhodes, S. O. Valind, P. Wollmer, and J. M. B. Hughes.** Regional lung density and blood volume in nonsmoking and smoking subjects measured by PET. *J. Appl. Physiol.* 63: 1324–1334, 1987.
6. **Brudin, L. H., S. O. Valind, C. G. Rhodes, D. R. Turton, and J. M. B. Hughes.** Regional lung hematocrit in humans using positron emission tomography. *J. Appl. Physiol.* 60: 1155–1163, 1986.
7. **Bryan, A. C., J. Milic-Emili, and D. Pengelly.** Effect of gravity on the distribution of pulmonary ventilation. *J. Appl. Physiol.* 21: 778–784, 1966.
8. **Glenny, R. W., W. J. Lamm, R. K. Albert, and H. T. Robertson.** Gravity is a minor determinant of pulmonary blood flow distribution. *J. Appl. Physiol.* 71: 620–629, 1991.
9. **Hakim, T. S., R. Lisbana, and G. W. Dean.** Gravity-independent inequality in pulmonary blood flow in humans. *J. Appl. Physiol.* 63: 1114–1121, 1987.
10. **Hubmayr, R. D., J. R. Rodarte, B. J. Walters, and F. M. Tonelli.** Regional ventilation during spontaneous breathing and mechanical ventilation in dogs. *J. Appl. Physiol.* 63: 2467–2475, 1987.
11. **Hughes, J. M. B.** Distribution of pulmonary blood flow. In: *The Lung: Scientific Foundations,* edited by R. G. Crystal, J. B. West, P. J. Barnes, N. S. Cherniack, and E. R. Weibel. New York: Raven, 1991, p. 1135–1145.
12. **Kaneko, K., J. Milic-Emili, M. B. Dolovich, A. Dawson, and D. V. Bates.** Regional distribution of ventilation and perfusion as a function of body position. *J. Appl. Physiol.* 21: 767–777, 1966.
13. **Michels, D. B., and J. B. West.** Distribution of pulmonary ventilation and perfusion during short periods of weightlessness. *J. Appl. Physiol.* 45: 987–998, 1978.
14. **Milic-Emili, J.** Static distribution of lung volumes. In: *Handbook of Physiology. The Respiratory System. Mechanics of Breathing.* Bethesda, MD: Am. Physiol. Soc., 1986, sect. 3, vol. III, pt. 2, chapt. 31, p. 561–574.
15. **Otis, A. B., C. B. McKerrow, R. A. Bartlett, J. Mead, M. B. McIlroy, N. J. Selverstone, and E. P. Radord.** Mechanical factors in distribution of pulmonary ventilation. *J. Appl. Physiol.* 8: 427–443, 1951.
16. **Phelps, M. E., E. J. Hoffman, S. C. Huang, and D. E. Kuhl.** ECAT: a new computerized tomographic imaging system for positron-emitting radiopharmaceuticals. *J. Nucl. Med.* 19: 635–647, 1978.
17. **Rhodes, C. G., S. O. Valind, L. H. Brudin, P. E. Wollmer, T. Jones, P. D. Buckingham, and J. M. B. Hughes.** Quantification of regional $\dot{V}/\dot{Q}$ ratios in humans by use of PET. II. Procedure and normal values. *J. Appl. Physiol.* 66: 1905–1913, 1989.
18. **Rhodes, C. G., P. Wollmer, F. Fazio, and T. Jones.** Quantitative measurement of regional extravascular lung density using positron emission and transmission tomography. *J. Comput. Assisted Tomogr.* 5: 783–791, 1981.
19. **Salazar, E., and J. H. Knowles.** An analysis of pressure-volume characteristics of the lungs. *J. Appl. Physiol.* 19: 97–104, 1964.
20. **Snashall, P. D., S. J. Keyes, B. Morgan, B. Jones, and K. Murphy.** Regional extravascular and interstitial lung water in normal dogs. *J. Appl. Physiol.* 49: 547–551, 1980.
21. **Valind, S. O., C. G. Rhodes, L. H. Brudin, and T. Jones.** Measurements of regional ventilation pulmonary gas volume: theory and error analysis, with special reference to positron emission tomography. *J. Nucl. Med.* 32: 1937–1944, 1991.
22. **Valind, S. O., C. G. Rhodes, and B. Jonson.** Quantification of regional ventilation in humans using a short-lived radiotracer. Theoretical evaluation of the steady-state model. *J. Nucl. Med.* 28: 1144–1154, 1987.
23. **Vawter, D. L., F. L. Matthews, and J. B. West.** Effect of shape and size of lung and chest wall on stresses in the lung. *J. Appl. Physiol.* 39: 9–17, 1975.
24. **West, J. B., and F. L. Matthews.** Stresses, strains and surface pressures in the lung caused by its weight. *J. Appl. Physiol.* 32: 332–345, 1972.
25. **Wollmer, P., C. G. Rhodes, R. M. Allan, A. Maseri, and F. Fazio.** Regional extravascular lung density and fractional pulmonary blood volume in patient with chronic pulmonary venous hypertension. *Clin. Physiol. Oxf.* 3: 241–256, 1983.